Auxetic Metamaterial Optimisation for Head Impact Mitigation in American Football

Benjamin Hanna, Rhosslyn Adams, Scott Townsend, Michael Robinson, Shwe Soe, Matthew Stewart, Peter Theobald *

Dr. B. Hanna, R. Adams, Dr. S. Townsend, Dr. M. Robinson, Dr. P, Theobald.
Cardiff School of Engineering, Cardiff University, Cardiff, UK.
E-mail: TheobaldPS@Cardiff.ac.uk

Dr. S. Soe.
Engineering, Design & Mathematics, University of West of England, Bristol. UK.

M. Stewart.
Charles Owen, Wrexham, UK.

Acknowledgements

This research was funded in part by the Head Health Challenge III. Prof Roy Burek (Charles Owen) was an important part of the wider team that initiated this work. His untimely passing has increased our commitment to progressing this technically demanding research area.

Abstract.

American football has a comparatively high rate of sports-related concussions, despite mitigating strategies including the use of protective helmets. The traditional energy absorbing component, elastomeric foam pads, have limited scope for leveraging any further protection. Alternative structures and materials that exhibit novel deformation mechanics have been proposed as a route to increased energy absorption capacity. This study investigated a metamaterial based on the Miura Ori folding pattern. Twenty-seven geometric combinations were designed and additively manufactured using commercially available thermoplastic polyurethane, before being impacted at multiple velocities. The Taguchi array provided insight into the theoretical behaviour of multiple additional variants. An optimised geometry was then proposed, which reduced linear accelerations across the test conditions and performed favourably when compared to current, elastomeric foam solutions. This work provides a promising foundation for future investigation.

Keywords: auxetic, metamaterial, impact absorption, head injury, structural optimization.

1. Introduction

Sport governing bodies are introducing new strategies to reduce head impact incidence and severity. Law changes in rugby union now mandate against any head contact, while sports involving frequent head impacts (e.g. soccer) are modifying training protocols. American football (hereafter termed 'football') aims to change play and improve protective equipment, encouraging innovative technologies to replace elastomeric foams as the primary mechanism of impact energy absorption. This study investigates a series of novel material-structures, in a quest to identify a high-performance solution.

Head injuries in football account for 21% of all injuries, a rate comparable to other contact sports, though 4.5-fold higher than the sector average.[1] Football causes 47% of high school sports-related concussions, with male college football producing more concussions than the totality of the next three high-risk sports: male ice hockey and lacrosse, and female soccer.[2, 3]. Strategies that reduce head peak linear acceleration are linked to decreased concussion risk. Reducing accelerations from 165g to 109g was estimated to reduce risk from 10% to 1%.[4] This relationship is consistent with other severity injury metrics such as the head injury criterion and rotational accelerations.[5]

Elastomeric foam is the conventional material employed to reduce head injury risk, with the impact performance defined by the base material and density of the homogeneous structure. Properties of the former influences cell wall strength and the buckling load or, in closed-cell structures, the onset of face-stretching. Foam provides highly efficient absorption when the impact magnitude and directionality can be precisely specified; however, where conditions vary, lower-energy impacts would not initiate microstructural deformation, while excessive force causes structural collapse and densification. Both scenarios would offer ineffective protection. These attributes fundamentally limit improving foam performance, meaning

59 innovative protective solutions now utilise new materials and structures as either additional or
60 replacement components.[6-8]

61 Additive manufacturing (AM) enables the use of lattice and surface-based cellular structures,
62 with the potential to introduce complex geometries that are impossible to realise using
63 traditional fabrication techniques. Cellular structures have great potential to achieve a tuned
64 mechanical response given their multiple geometric parameters, so offering a particularly
65 promising route to out-perform elastic foams.[9-11] Auxetic materials (i.e. with a negative
66 Poisson's ratio) have demonstrated favourable energy absorption performance.[12, 13] They
67 have also demonstrated synclastic curvature – controllable curvature in two planes, making
68 them ideal for integration into helmets.[14] One such approach is adopting the Miura-Ori
69 (MO) folding pattern, which affords a tailored structural design for effective energy
70 absorption.[15, 16] Construction from a thermoplastic polyurethane has also shown
71 promising behaviour in football-related loading conditions.[17]

72 Employing additive manufacturing enables new design creativity; however, such scope also
73 means it is challenging to identify the structural design that achieves optimal performance.
74 Whilst experiment-based optimisation techniques have proven effective in the literature when
75 applied to impact design,[18] the Taguchi method requires relatively few tests, considers part
76 variability (i.e. 'signal-to-noise') and has been employed optimising AM design and impact
77 protection systems.[19, 20]
78 This paper now seeks an optimal MO geometry to minimise the peak linear acceleration
79 (PLA) at three football-related impact velocities. Success would create potential to reduce
80 head injury risk.

2. Materials and Methods

2.1. Methods

A nominal MO unit cell was interrogated to reveal 7 structural parameters that influence geometry (**Figure 1**). Four parameters were then selected for further investigation based on the potential to influence the MO's impact absorption performance: Chevron Angle (α), Interior Intersection Angle (β), Exterior Intersection Angle (γ), and Wall Thickness (t). These parameters then had 6 potential interactions: α – β; α – γ; α – t; γ – β; γ – t; β – t.

Cell Height (H) was unconstrained due to its dependence on β and γ. Cell Depth (D) and Length (L) directly influenced cell volume and so were considered control variables. The former was defined as 30mm, to be consistent with a typical energy-absorbing helmet liner thickness. Length L was defined as 15.8mm, ensuring consistency with published MO geometries [14]. The final unit cell was proliferated through 60 x 60 x 30 (i.e. D) mm^3.

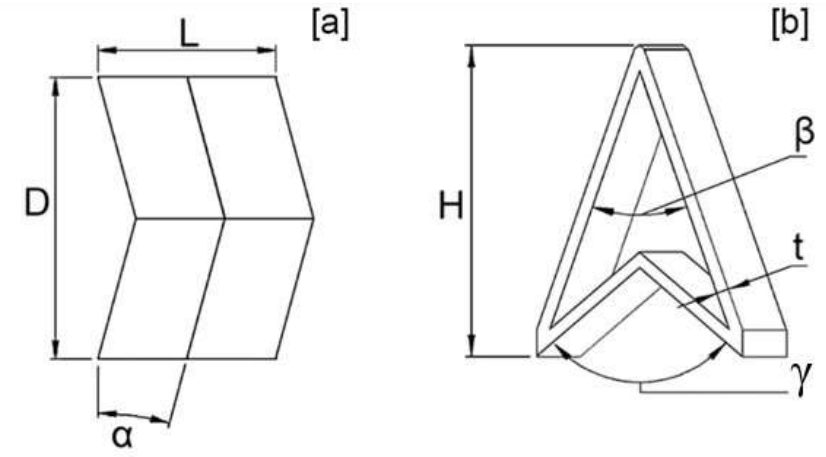

Figure 1: The structural parameters that influence MO cell geometry. [a] Frontal view. [b] Top view.

Three 'levels' were then defined for each of the 4 parameters, describing a minimum (level 1), midpoint (level 2) and maximum (level 3) value. Midpoints for angles γ and β were adopted from an MO structure previously described for head protection applications,[17] with upper and lower bounds selected to maximise the potential design space whilst retaining the

distinct ‘arrowhead’ design. The t midpoint was defined by the literature, with upper and lower bounds governed by manufacturing constraints. Angle α was minimised, as smaller values achieve favourable performance.[21] These ranges are presented in **Table 1**.

Table 1: Parameter levels used for optimisation.

Parameter	Level 1	Level 2	Level 3
α [°]	1	5	9
γ [°]	80	110	140
β [°]	33	38	43
t [mm]	0.6	0.9	1.2

This approach creates 81 unique unit cells; however, mass-scale manufacture and testing are time-intensive. Selecting a representative sample was enabled by adopting the Taguchi method. Taguchi’s L27 array was the smallest array that could accommodate the placement of the four parameters and the six interactions. Adopting this array systematically identified 27 parametric combinations for further investigation (Table 2). Extrapolating these data would ultimately identify the most effective solution from the 81 potential structures.

Table 2: Parameters defining the 27 unique MO unit cells, generated using the Taguchi method.

Structure	**α [°]**	**γ [°]**	**β [°]**	**t [mm]**
CH01	1	80	33	0.6
CH02	1	80	38	0.9
CH03	1	80	43	1.2
CH04	1	110	33	0.9
CH05	1	110	38	1.2
CH06	1	110	43	0.6
CH07	1	140	33	1.2
CH08	1	140	38	0.6
CH09	1	140	43	0.9

CH10	5	80	33	0.9
CH11	5	80	38	1.2
CH12	5	80	43	0.6
CH13	5	110	33	1.2
CH14	5	110	38	0.6
CH15	5	110	43	0.9
CH16	5	140	33	0.6
CH17	5	140	38	0.9
CH18	5	140	43	1.2
CH19	9	80	33	1.2
CH20	9	80	38	0.6
CH21	9	80	43	0.9
CH22	9	110	33	0.6
CH23	9	110	38	0.9
CH24	9	110	43	1.2
CH25	9	140	33	0.9
CH26	9	140	38	1.2
CH27	9	140	43	0.6

Each structure was then designed as a 60 x 60 x 30 mm flat sample using Solidworks computer-aided design (CAD) software (Dassault Systems, France). An exemplar part is presented in Figure 2. Testing flat material samples, as opposed to the material assembled within a helmet system, allows for direct performance comparison and is independent of factors including curvature and shell stiffness. An identical approach has been reported by other authors.[22-24] All designs were then exported to Simplify3D (Simplify3D, US), an advanced AM slicing platform. Each sample was manufactured via fused filament fabrication (2017 Flashforge Creator Pro printer), retrofitted with high-specification extrusion control (Diabase Engineering, USA). All samples were manufactured from Cheetah, a commercially available thermoplastic polyurethane (NinjaTek, USA), using process parameters reported in Hanna.[25] Cheetah characterisation data has previously been reported in Robinson,[26] with the Prony coefficients from stress relaxation experiments

126 presented in Table 3. Equally sized elastomeric foam samples were cut from two off-the-
127 shelf American football helmets ('helmet 1' and 'helmet 2'), to provide comparative
128 measures.

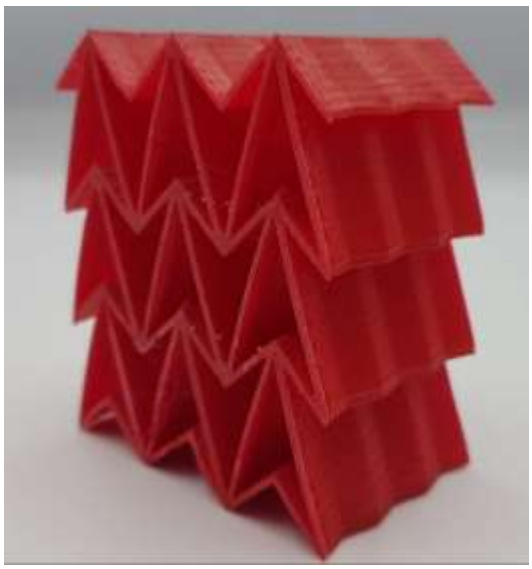

129

130 **Figure 2**: A photograph presenting one of the MO structures, generated via the Taguchi
131 process.

132 **Table 3:** Cheetah Prony coefficients, represented from [26]

	G /MPa	K /MPa	tau /s
1	0.477	0.0000	1.21E-02
2	0.125	0.0000	15.82

133

134 **2.2. Methods**

135 Each sample was investigated in an impact test machine (Dynatup 9250HV; Instron, US). A
136 flat, 4.8kg rigid impactor struck each sample 5 times, resting for 75 ± 15 s between impacts.
137 This setup is schematically described in Figure 3. Data was recorded with a 500g single axis
138 linear accelerometer (Honeywell, US) via a data acquisition system at 500Hz, before being
139 smoothed using a Butterworth filter, adopting a 1 kHz cut off frequency. Acceleration-time
140 traces were considered once exceeding 4g, to achieve comparison across all data. This is the

141 approach adopted by the NOCSAE testing standards, to eliminate potential sources of noise
142 from the test equipment.
143
144 Each sample was exposed to impacts at three different velocities, derived from the literature.
145 Velocities associated with injurious football collisions have previously been reported as 5.5,
146 7.4 and 9.3ms^{-1}.[5, 27] It is recognised, however, that some impact energy is dissipated
147 through the neck, meaning velocities applied via rigid test apparatus should be scaled by 0.6
148 to accurately represent such collisions.[5] Applied to this study, samples were initially tested
149 at 3.30 ms^{-1}, then after 24 hours rest for inspection and full relaxation at 4.44 ms^{-1} and then,
150 following a further 24 hours rest, 5.58 ms^{-1}. The mean peak linear acceleration (PLA) for
151 each velocity was then calculated, before computing the 3 velocity score (3VS), adopted from
152 the new football helmet assessment method.[28]

153 $$3VS = 0.06737PLA_{3.30} + 0.04167\mathrm{PLA}_{4.44} + 0.05442PLA_{5.58} \quad \text{(eqn 1)}$$

154

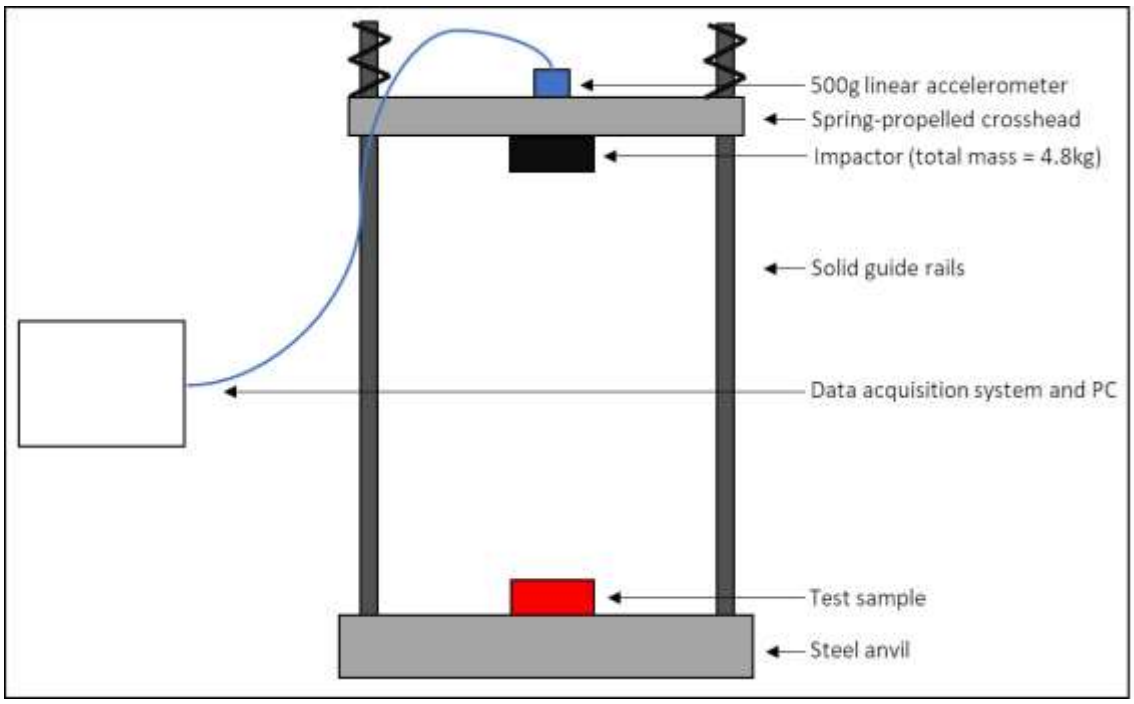

155

156 **Figure 3**: Schematic representation of the impact test setup.

157 *2.2.1. Array-based Analysis*

158 Established Taguchi techniques were then employed to statistically extrapolate the
159 experimental data, identifying the optimal structure from the 81 possible geometric
160 combinations. The mean standard deviation (MSD, eqn 2) was calculated for each sample, at
161 each impact velocity.

162 $$MSD = \frac{\sum_{i=1}^{i=n} x_i^2}{n} \quad \text{(eqn 2)}$$

163 where n is the number of datapoints and x_i is the ith data point. From the MSD, a signal to
164 noise ratio (S/N) was calculated, using equation 3.

165 $$S/N = -10 \cdot \log_{10}(MSD) \quad \text{(eqn 3)}$$

166 To calculate each parameter's influence, samples were then grouped by level for the
167 parameter studied, and the average S/N value was calculated. For example, the average
168 response where α = 5° is calculated from the S/N values of samples CH10 - 18. This was
169 repeated for each parameter level, calculating the average S/N value. The mean response of
170 all samples is plotted to quantify parametric influence, in a Main Effects plot.
171
172 Interactions between the geometric parameters were identified using surface plots. Given
173 four parameters with three levels, 81 possible structural combinations could be developed.
174 The surface plot describes the nature of the relationships between the two parameters.
175
176 An ANOVA then calculated the contribution of each geometric parameter to a structure's
177 overall response.

3. Results.

3.1. Baseline Experimental Analysis:

All 27 parametric combinations were manufactured from Cheetah. These manufactured parts were consistently slightly heavier than forecast by the CAD data (2.45 ± 1.35g). All samples were struck by the impact test machine as per the above protocol, with acceleration-time traces collected for each impact. Selected traces are presented in **Figure 4** from across the 3 impact velocities. These traces represent the structure that achieved the lowest PLA (i.e. most favourable response) and that which recorded the highest PLA, due to being either too stiff or soft.

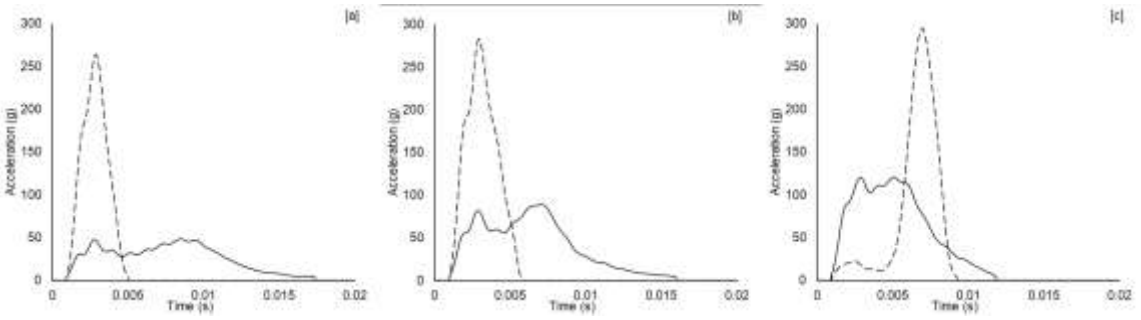

Figure 4: Selected acceleration-time plots drawn from the 3 impact velocities, representing the lowest (solid) and highest (dashed) PLA values. [a] 3.30 m/s; lowest PLA = CH03, highest PLA = CH06. [b] 4.44 m/s; lowest PLA = CH13, highest PLA = CH17. [c] 5.56 m/s; lowest PLA = CH16, highest PLA = CH06.

These data, plus the average PLA across all 27 samples for each impact condition, were then plotted against established head injury thresholds, to gain an appreciation of their performance (Figure 5a). Comparison to commercially available helmet foam is also presented (Figure 5b).

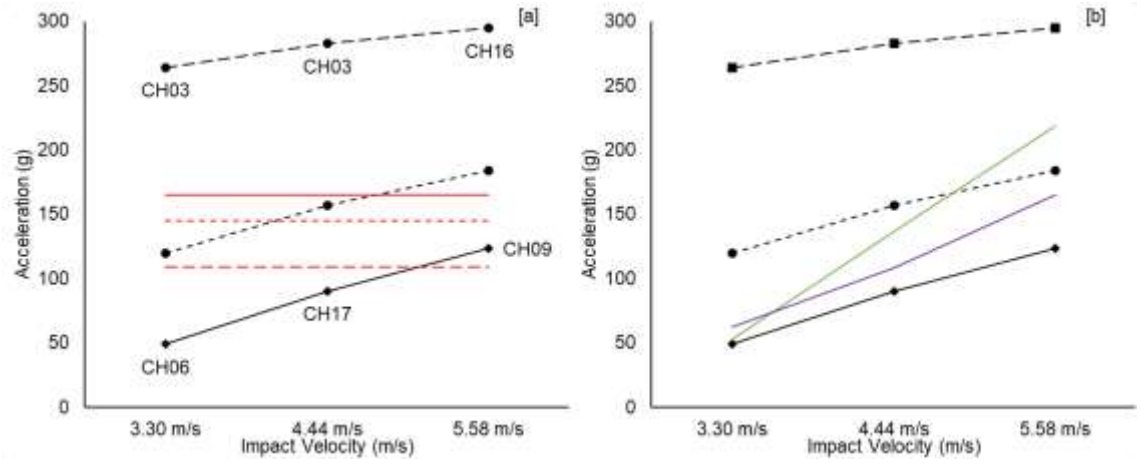

196

197 **Figure 5**: Peak linear accelerations for best performing (solid), worst performing (dashed)
198 and average (dotted) L27 samples, across the 3 impact velocities. **[a]** Solid red line = 10%
199 SRC risk; dotted red line = 5% SRC risk; dashed red line = 1% SRC risk. **[b]** Green line =
200 *helmet 1* elastomeric foam; Purple line = *helmet 2* elastomeric foam.

201 **3.2. Array-based Analysis**

202 The 3VS was calculated for each structure using equation 1. A Main Effects plot assessed
203 the influence of parameters and interactions on the PLA (**Figure 6**). A horizontal trend
204 indicates PLA is independent of a specific parameter, whilst a trend with significant variation
205 indicates the parameter influences sample performance. The lowest PLA represents the most
206 favourable response. Whilst all parameters and interactions have some influence on the
207 structural performance, t is the most influential.

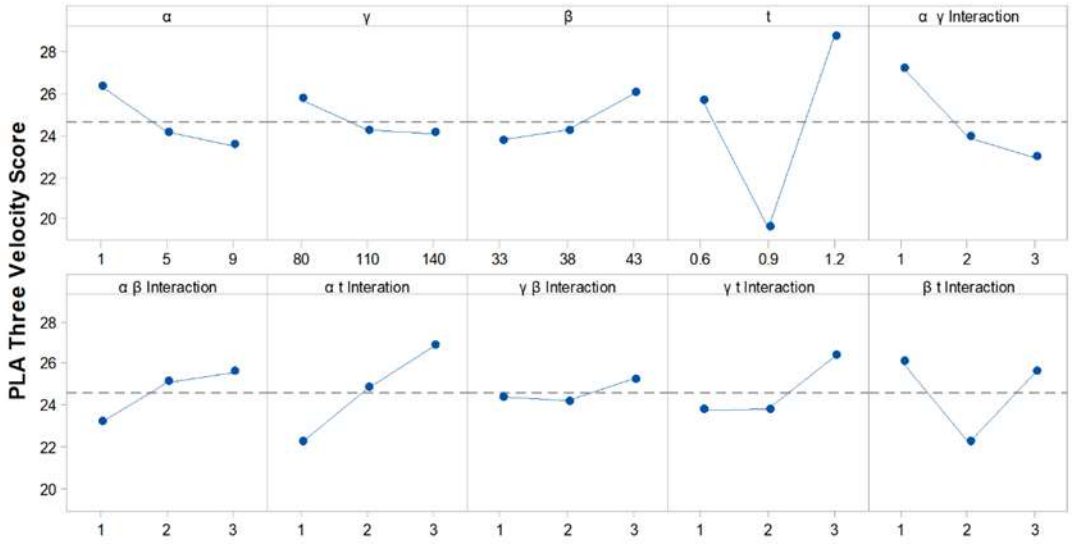

Figure 6: Main Effects plots describing the influence of the geometric parameters and the interactions on the structural performance, measured via the peak linear acceleration (PLA).

The 6 interactions are further evaluated in the Interaction Surface Plot, **Figure 7**. A surface with parallel contours denotes no interaction between two parameters. Diverging contours indicate weak interaction, whereas strong interaction appears as a complex surface with no consistent directionality. It is observed that interactions containing t are less complex, though produce greater variation (i.e. Fig 7b, d and f).

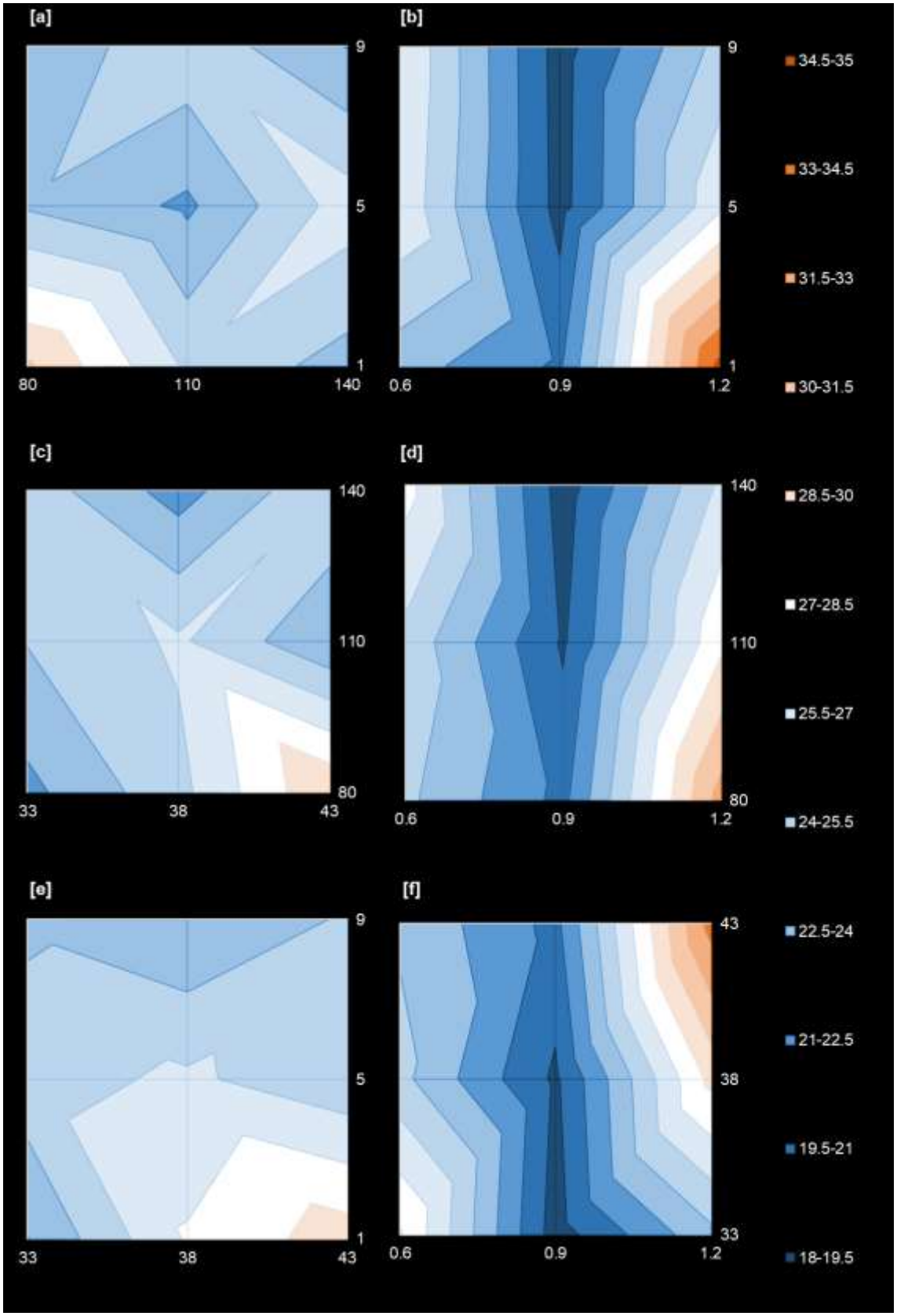

Figure 7: Interaction Surface Plots for 3VS, [a] α-γ Interaction, [b] α-t Interaction, [c] β-γ Interaction, [d] γ-t Interaction, [e] α-β Interaction, [f] β-t Interaction.

The ANOVA identified design parameters with a statistically significant influence on performance (**Table 4**), supporting the relationships exhibited in Figure 6 and Figure 7.

Table 4: ANOVA results for 3VS

Factor	Degrees of freedom	Sum of Squares	Variance	Contribution	F-Value	Significance 90% CI	Significance 95% CI
α	2	40.04	20.02	4.30%	1.47	No	No
t	2	394.82	197.41	42.37%	14.54	Yes	Yes
α γ Interaction	2	91.13	45.57	9.78%	3.36	Yes	No
α t Interaction	2	96.82	48.41	10.39%	3.56	Yes	No
γ t Interaction	2	39.71	19.86	4.26%	1.46	No	No
β t Interaction	2	79.23	39.61	8.50%	2.92	Yes	No
Error	14	190.12	13.58	20.40%			
Total	26	931.86		100.00%			

3.3. Final Design

The geometric parameters from the Main Effects plot with the lowest 3VS score produced the optimised design. The ANOVA and Interaction Surface Plots enabled design verification by considering the interaction performance of each parameter. The final design was then manufactured and tested according to the previously discussed impact method (**Figure 8**).

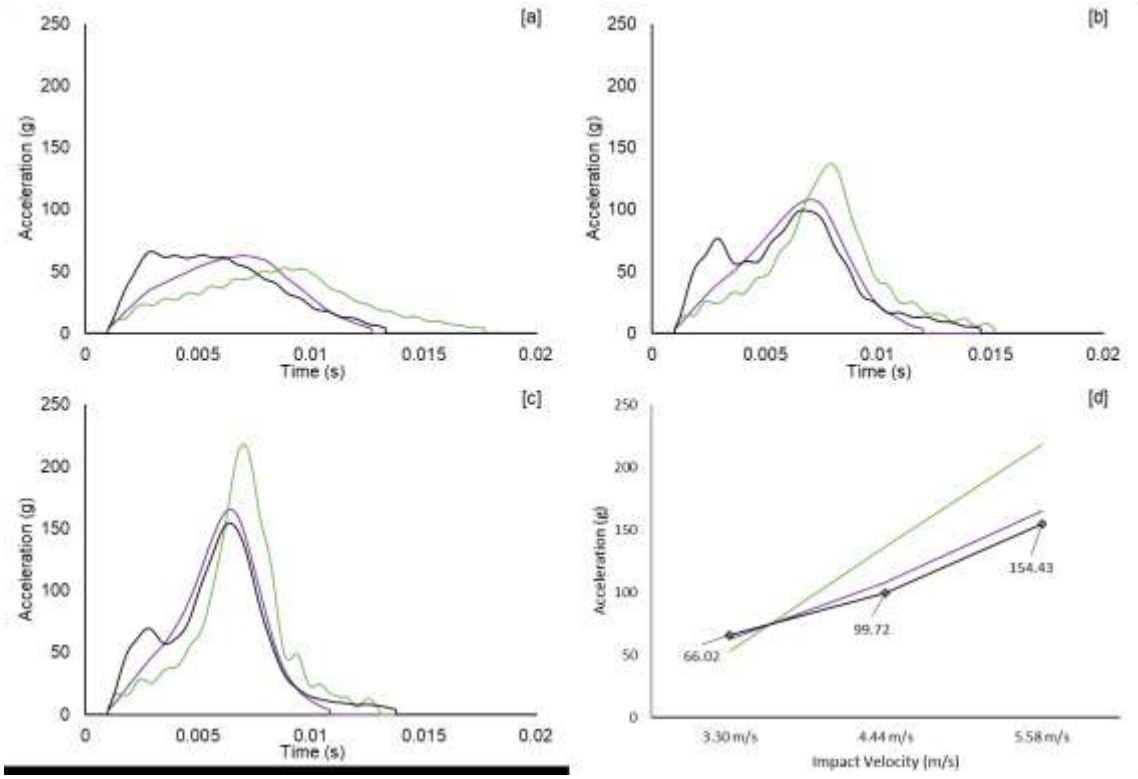

Figure 8: Acceleration-time plots comparing the optimised MO geometry (black line), *helmet 2* foam (blue line) and *helmet 1* foam (green line). [a] 3.30 m/s, [b] 4.44 m/s and [c] 5.58 m/s impacts. [d] summarised PLA data.

The optimised structure demonstrated superior performance at the two highest impact velocities relative to the comparator foams, with similar performance at the lowest speed. The MO sample exhibited a two-peak acceleration response at the highest velocities, with the latter peak caused by the onset of densification. The initial peak is attributed to the walls folding, which temporarily reduces acceleration. The optimal geometry produced a 3VS 19.5% lower than the *helmet 1* foam, and 4% lower than the *helmet 2* foam (**Table 5**).

Table 5: 3VS of optimal MO structure and two comparison foams.

Sample	Three Velocity Score (g)	Relative To Best Foam (%)
Helmet 2 foam	17.715	100
Helmet 1 foam	21.127	119.261
L27 Maximum	45.233	255.337
L27 Minimum	17.007	96.003

L27 Average	24.618	138.967
3VS Optimal	17.007	96.003

242

243

4. Discussion.

The MO structure was successfully optimised and achieved superior performance versus the comparator foams in the more severe collision scenarios. This innovation should, therefore, transfer less energy to the head during a football collision, potentially offering enhanced player protection.

The Taguchi optimisation strategy provided a robust route to understanding the geometric parameters and their relative interactions. Twenty-seven structures were designed, manufactured, and tested to enable analytical interrogation of 81 possible structural combinations. Wall thickness, t, was dominant in the 3VS response with 42% contribution to sample variation, with a further 23% contribution when interactions with the other parameters are considered. The dominant behaviour of t is linked to the adoption of a relatively large cell size, minimising the influence of manufacture inaccuracy and increasing control of non-examined parameters.[29] The optimal design achieved <1% sports-related concussion risk for the two lowest impact velocities and <10% risk at the highest velocity. Both helmet foams demonstrated reduced effectiveness at the highest impact velocity, the average velocity of concussion related impacts, suggesting the MO may be capable of reducing SRC prevalence within more severe football collisions.

MO performance also appears favourable relative to individual components, with lower PLA values relative to the Aware-Flow shock absorber at higher velocities.[8] Performance appears inferior when compared to some other systems tested in full helmet configurations, though further scope remains for improvement by varying the sample size, amongst other design considerations. The similar magnitudes of the *helmet 2* foam compared to previously reported helmet data provides confidence that this experimental setup broadly reflects in situ behaviour.[7]

Whilst none of the investigated angles had statistical significance in their primary effect, many interactions were significant, suggesting secondary effects. Designing relatively large cells may have constrained the metamaterial behaviour and underlying MO characteristics,[30] though reducing cell size would mean thinner walls and so a softer response prior to densification. A change to a stiffer TPU would allow for the further optimisation of cell wall thickness, while maintaining the elastic properties of the derived metamaterial necessary for the application. A stiffer material would also allow for reduced wall thickness whilst maintaining wall buckling, enabling a reduction in overall mass.

This study did not perform optimisation with respect to duration, meaning impact time could increase whilst achieving a reduced PLA. Considering the structures as flat slabs is consistent with past studies and reflects the common approach within football helmet design, where small flat pads are proliferated throughout the internal shell wall to achieve complete coverage. Such an approach is fundamental to understanding and evaluating new and innovative materials, before ultimate translation into a complete helmet assembly.

5. Conclusion

The MO geometry has demonstrated potential for use in football-related applications, as tuning the mechanical response has achieved superior performance versus contemporary materials. This provides a platform for future work to explore translation into a full helmet assembly and to consider load cases from other sports/environments.

References

1. Willigenburg, N.W., et al., *Comparison of Injuries in American Collegiate Football and Club Rugby: A Prospective Cohort Study.* Am J Sports Med, 2016. **44**(3): p. 753-60.
2. Marar, M., et al., *Epidemiology of concussions among United States high school athletes in 20 sports.* Am J Sports Med, 2012. **40**(4): p. 747-55.
3. Zuckerman, S.L., et al., *Epidemiology of Sports-Related Concussion in NCAA Athletes From 2009-2010 to 2013-2014: Incidence, Recurrence, and Mechanisms.* Am J Sports Med, 2015. **43**(11): p. 2654-62.
4. Funk, J.R., et al., *Biomechanical risk estimates for mild traumatic brain injury.* Annu Proc Assoc Adv Automot Med, 2007. **51**: p. 343-61.
5. Viano, D.C., C. Withnall, and D. Halstead, *Impact performance of modern football helmets.* Ann Biomed Eng, 2012. **40**(1): p. 160-74.
6. Breedlove, K.M., et al., *The Ability of an Aftermarket Helmet Add-On Device to Reduce Impact-Force Accelerations During Drop Tests.* Journal of Athletic Training, 2017. **52**(9): p. 802-808.
7. Johnston, J.M., et al., *Simulation, fabrication and impact testing of a novel football helmet padding system that decreases rotational acceleration.* Sports Engineering, 2015. **18**(1): p. 11-20.
8. KrzeminskI, D.E., et al., *Investigation of linear impact energy management and product claims of a novel American football helmet liner component.* Sports Technology, 2011. **4**(1-2): p. 65-76.
9. Bertoldi, K., et al., *Flexible mechanical metamaterials.* Nature Reviews Materials, 2017. **2**(11): p. 17066.

10. Fathers, R.K., J.M. Gattas, and Z. You, *Quasi-static crushing of eggbox, cube, and modified cube foldcore sandwich structures.* International Journal of Mechanical Sciences, 2015. **101-102**: p. 421-428.
11. Soe, S.P., et al., *Feasibility of optimising bicycle helmet design safety through the use of additive manufactured TPE cellular structures.* The International Journal of Advanced Manufacturing Technology, 2015. **79**(9): p. 1975-1982.
12. Foster, L., et al., *Application of Auxetic Foam in Sports Helmets.* Applied Sciences, 2018. **8**(3): p. 354.
13. Lisiecki, J., et al., *Tests of polyurethane foams with negative Poisson's ratio.* physica status solidi (b), 2013. **250**(10): p. 1988-1995.
14. Duncan, O., et al., *Review of Auxetic Materials for Sports Applications: Expanding Options in Comfort and Protection.* Applied Sciences, 2018. **8**(6): p. 941.
15. Schenk, M., S.D. Guest, and G.J. McShane, *Novel stacked folded cores for blast-resistant sandwich beams.* International Journal of Solids and Structures, 2014. **51**(25): p. 4196-4214.
16. Zhang, J., et al., *Quasi-static large deformation compressive behaviour of origami-based metamaterials.* International Journal of Mechanical Sciences, 2019. **153-154**: p. 194-207.
17. Robinson, M., et al. *Developing elastomeric cellular structures for multiple head impacts*. in *IRCOBI*. 2017. Antwerp, Belgium.
18. Forsberg, J. and L. Nilsson, *Evaluation of response surface methodologies used in crashworthiness optimization.* International Journal of Impact Engineering, 2006. **32**(5): p. 759-777.

19. Sood, A.K., R.K. Ohdar, and S.S. Mahapatra, *Parametric appraisal of mechanical property of fused deposition modelling processed parts.* Materials & Design, 2010. **31**(1): p. 287-295.
20. Srivastava, M. and S. Rathee, *Optimisation of FDM process parameters by Taguchi method for imparting customised properties to components.* Virtual and Physical Prototyping, 2018. **13**(3): p. 203-210.
21. Harris, J., *Additively manufactured metallic cellular materials for blast and impact mitigation*, in *Department of Engineering*. 2017, Cambridge University.
22. Adams, R., et al., *A novel pathway for efficient characterisation of additively manufactured thermoplastic elastomers.* Materials & Design, 2019. **180**: p. 107917.
23. Robinson, M., et al., *Mechanical characterisation of additively manufactured elastomeric structures for variable strain rate applications.* Additive Manufacturing, 2019. **27**: p. 398-407.
24. Townsend, S., et al., *3D printed origami honeycombs with tailored out-of-plane energy absorption behavior.* Materials & Design, 2020. **195**: p. 108930.
25. Hanna, B., *Development of a metamaterial for use in American football head protection.* 2020: Cardiff University.
26. Robinson, M., *Developing novel materials to enhance motorcyclist safety*. 2019: Cardiff University.
27. Viano, D.C. and D. Halstead, *Change in size and impact performance of football helmets from the 1970s to 2010.* Ann Biomed Eng, 2012. **40**(1): p. 175-84.
28. Biocore. *Helmet test protocol*. 2019 Accessed 28th June 2021].
29. Bikas, H., A.K. Lianos, and P. Stavropoulos, *A design framework for additive manufacturing.* The International Journal of Advanced Manufacturing Technology, 2019. **103**(9): p. 3769-3783.

30. Schenk, M. and S.D. Guest, *Geometry of Miura-folded metamaterials.* Proceedings of the National Academy of Sciences, 2013. **110**(9): p. 3276-3281.